A Novel Speckle Reducing Scan Conversion in Ultrasound Imaging System

Dipannita Ghosh, Debashis Nandi, Palash Ghosal and Amish Kumar

Abstract Quality of ultrasound image is dominantly limited by two major issues such as low resolution and speckle noise. The existing speckle reduction techniques are mostly applied either before or after scan conversion. Filtering before scan conversion results in huge computational load since the amount of data handled is quite large while filtering after scan conversion provides poor image quality. In this paper, a novel and computationally efficient filtering technique has been proposed where filtering is performed along with scan conversion using spatial linear adaptive and nonlinear filters in two directions of scan conversion geometry. The proposed framework is found suitable for the real-time applications and improves the visual quality of the image. Quality metrics for the proposed method have been compared to other existing methods to show the novelty of the work.

Keywords Ultrasound image · Scan conversion · Speckle reduction

1 Introduction

Ultrasound imaging modality is predominantly used as a diagnostic tool in modern medicine. It is a noninvasive means of examining body's internal organs and is practically risk-free to human body. The quality of the ultrasound image is largely affected by a prominent factor known as speckle noise. Speckle is an inherently generated

D. Ghosh (✉) · D. Nandi · P. Ghosal · A. Kumar
Department of Information Technology, National Institute of Technology,
Durgapur 713209, West Bengal, India
e-mail: dipannitaghosh21@gmail.com

D. Nandi
e-mail: debashisn2@gmail.com

P. Ghosal
e-mail: ghosalpalash@gmail.com

A. Kumar
e-mail: amishkumar562@gmail.com

P.K. Sa et al. (eds.), *Progress in Intelligent Computing Techniques: Theory, Practice, and Applications*, Advances in Intelligent Systems and Computing 518,
DOI 10.1007/978-981-10-3373-5_34

noise by the ultrasound imaging acquisition system degrading resolution and contrast of the image. Speckle appears as a granular pattern [1] originating from a waveform with various independent scattered components. It seems as bright and dark spots over the surface of the image and brings difficulties to experts in medical diagnosis. Thus, speckle reduction becomes a rising area of research in order to make the ultrasound imaging modality comparable to the other medical imaging practices in terms of image excellence. In ultrasound imaging system, speckle noise is generally suppressed at the preprocessing stage or at the post-processing stage. The existing noise reduction filtering techniques [2–11] are, therefore, mostly applied either on the raw scan data (i.e., before scan conversion) or on the scan-converted images (i.e., after scan conversion). Filtering on raw scan data generates huge computational load whereas filtering after scan conversion lacks in image quality as information content in image hampers largely during scan conversion. Consequently, a new efficient speckle reduction technique is proposed which unifies filtering and scan conversion simultaneously, i.e., filtering along with scan conversion. The resultant image of filtering scan conversion is the outcome of filtering separately in the two directions of scan conversion geometry: radial direction and horizontal direction. The choice of filter can be made different in the two directions of scan conversion filtering. The present article, therefore, has investigated the performance of the speckle filtering scan conversion using either same or different combinations of linear and nonlinear filters imposed in two different phases of scan conversion.

2 Noise Model

The noise embedded to the ultrasound scan lines is the combined form of speckle and Gaussian noise. Speckle is multiplicative in nature and generally assumed as Rayleigh distribution. This speckle noise is multiplied with the signal and then log-compressed by the logarithmic amplifier. As a result, the multiplied speckle noise becomes additive to the log-compressed signal at the output of the logarithmic amplifier. Afterward, the Gaussian noise is added to the logarithmic amplifier output for the simulation of the ultrasound scan lines that are made corrupted by speckle and Gaussian noise. The noisy signal is then scan-converted. The noisy scan data is thus modeled as

$$S_0(i,j) = S(i,j) + n_G(i,j) + n_s\, p(i,j)\ . \tag{1}$$

where $S(i,j)$ is the log-compressed signal, $n_G(i,j)$ is the additive Gaussian noise, and $n_s\, p(i,j)$ is the log-compressed speckle noise.

3 Speckle Reduction Methods

The existing speckle reduction methods can be broadly categorized as compounding techniques [12, 13], spatial linear adaptive and nonlinear filtering [3–7], multi-scale method [8–11], non-local means denoising [14, 15], and sparse representation-based denoising [16]. Lee filter [3], Kuan filter [5], Dutt and Greenleaf [7], Bamber and Daft [4] are the examples of linear spatial adaptive filters. These filters are based on local statistics and perform filtering within the fixed size window centering the pixel under consideration increasing smoothness in homogeneous region of the image. Median, weighted median, adaptive weighted median [6], and directional median [17] are some of the nonlinear filters useful for preserving edges in an image while reducing random noise. The homogeneity map method (HMM) is introduced [18] for speckle reduction based on the mapping of homogeneous and non-homogeneous regions of the speckled image. Again, optimized Bayesian NL-means with block selection (OBNLM) [15] uses the adaptation of non-local (NL) means using Bayesian formulation. It uses the Pearson distance for patch comparison for speckle reduction generating a competitive performance.

Scan conversion in ultrasound imaging system is conventionally done by interpolation method. In the proposed method, the interpolation is restored by filtering using some of the spatial linear and nonlinear speckle reduction filters and is also compared with the two competitive state-of-the-art methods such as HMM and OBNLM.

4 Proposed Method for Speckle Reduction Through Filtering Scan Conversion

The simplified schematic block diagram of a typical diagnostic B-mode ultrasound imaging system that employs filtering scan conversion is shown in Fig. 1. In filtering scan conversion framework, the reconstruction of image from noisy scan data is performed along two directions in two successive phases, respectively: (i) filtering scan conversion along radial direction (phase 1) and (ii) filtering scan conversion along horizontal direction (phase 2). The essential steps of the proposed filtering scan conversion algorithm for obtaining the rectangular grids have been discussed in detail below.

Phase 1

Aim: Computation of the values at the points where radial lines intersect with the horizontal grid lines marked with solid samples in Fig. 2a.
Assumption: Solid triangular points in scan conversion geometry (Fig. 2a) are the sample points.

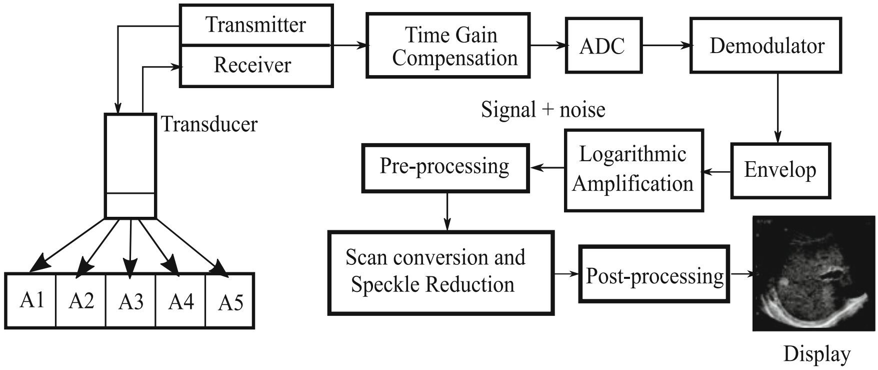

Fig. 1 Block diagram of ultrasound imaging system (speckle reduction is done with scan conversion)

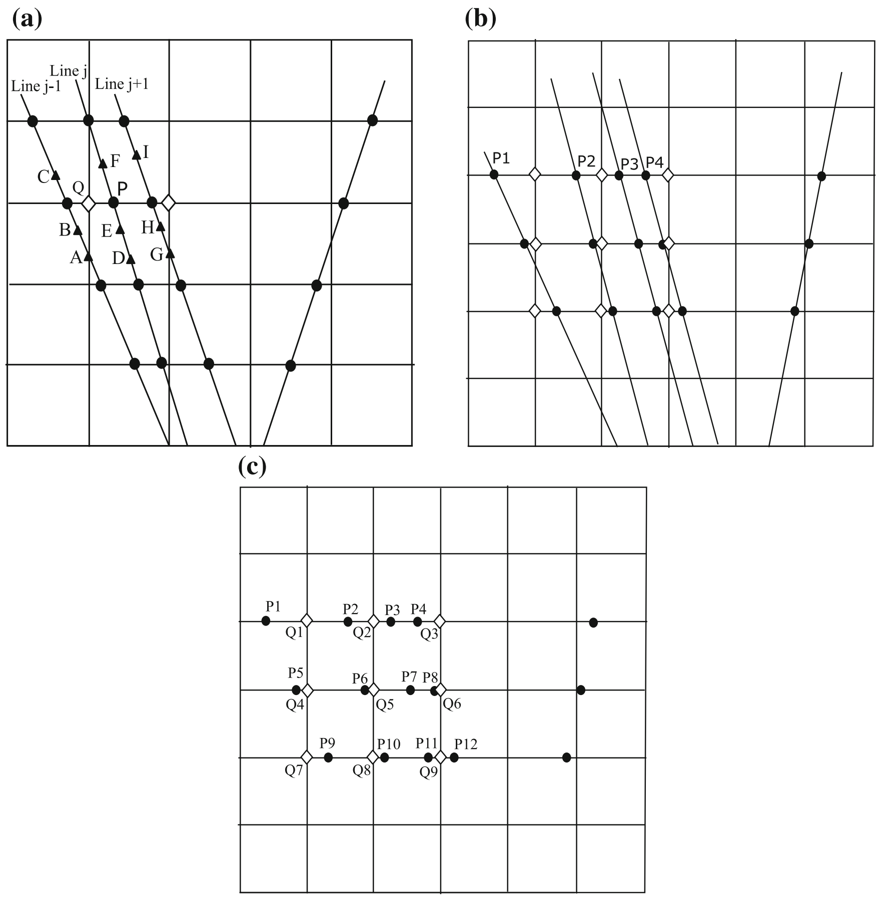

Fig. 2 **a** Scan conversion geometry **b** Geometry of first-stage computation **c** Pixel geometry for raster grid points computation

Steps

1. Consider three successive lines, Line j − 1, Line j, and Line j + 1.
2. P is considered as a point where the radial line, i.e., Line j cuts the horizontal grid line.
3. Find the nine surrounding nearest points around P.
4. A, B, C, D, E, F, G, H, and I are the nearest points around P along Line j − 1, Line j, and Line j + 1. E is the nearest along Line j termed as s(nearest,j).
5. To calculate the pixel value at P, these nine samples around point P are considered as a member of local window.
6. Use any spatial linear or nonlinear filters to find P. To adapt Kuan filter [5], the following equation is used

   $$p = \bar{s} + k[\theta_r - \bar{s}]\ . \tag{2}$$

   where $\bar{s}$ is the average value of the pixels within the local window and θ_r is the interpolated value at the desired point P on the jth scan line for rth-order interpolation. The parameter k can be determined from the equation below

   $$k = \frac{Var(x)}{Var(x) + \bar{x}^2 + Var(x)}\ . \tag{3}$$

   where $\bar{x}$ and $Var(x)$ represent the mean and variance of local window, respectively. The interpolated value can be taken as $\theta_r = s(nearest, j)$, i.e., nearest neighbor $(or\ zeroth - order\ interpolated\ value)$.
7. Find all the points where radial lines cut the horizontal grid lines by moving the window along the scan lines. P1, P2, and P3 are such points as shown in Fig. 2b.

The geometry will be then converted as shown in Fig. 2c. Now, with the help of available points P1, P2, and P3, the raster grid points of the raster scan are computed. It can be illustrated with the help of Fig. 2c.

Phase 2

Aim: Computation of the pixel values at the grid points of the Cartesian coordinates (i.e., where vertical grid line cuts the horizontal grid lines) from the computed values of the previous step. Pixel values at raster grid points Q1, Q2, and Q3 (Fig. 2c) are to be computed.

Steps

1. Consider the raster grid point Q5 in the ith row and jth column. Find three nearest points of Q5 along ith row.
2. P7, P6, and P8 are such three nearest points. P7 is the nearest one assigned as p(i,nearest).
3. Find three nearest points from previous and next rows, i.e., $(i - 1)$th row and $(i + 1)$th row.
4. Find the grid point Q2 of the same column and $(i - 1)$th row and search three points around Q2 along the row. In a similar way, three nearest points from next row, i.e., $(i + 1)$th row can be found out.

5. Finally, the pixel point at the grid point Q5 can be computed from these nine points by using similar type of Eq. 2

$$q = \bar{p} + k[\phi_r - \bar{p}]\ . \quad (4)$$

where $\bar{p}$, ϕ_r indicate the same meaning as of $\bar{s}$, ϕ_r in Eq. 2. The final pixel values at the grid point are evaluated by moving the window along horizontal direction.

In the proposed method, filtering can be performed in two different manners: FSC (2 pass) and FSC (1 pass). When filtering is performed in both the radial and horizontal directions, the technique is known as speckle reduction through filtering scan conversion in two pass (FSC (2 pass)). After computation of the point P, the raster grid point can also be computed by simple linear interpolation. This technique is termed as speckle reduction through filtering scan conversion in single pass (or FSC (1 pass)).

5 Simulation and Results

The efficiency of the algorithm has been evaluated by generating phantom data from analytic function $f(x, y) = \frac{1}{4}[\sin(wx)]$, placing few holes of different sizes. The simulations were performed in MATLAB and were tested in Windows 7 Home Basic, Intel(R) Core(TM) i5-4690 CPU @ 3.50 GHz processor, 4 GB RAM, 32-bit OS, with 500 GB hard disk.

The scan lines of the raw scan data are corrupted with the three levels of speckle and Gaussian combined parameters, speckle ($\sigma = 1.0$) with 20 dB Gaussian noise (overall noise = 17.6 dB), speckle ($\sigma = 1.5$) with 15 dB Gaussian noise (overall noise = 12.6 dB), and speckle ($\sigma = 2.0$) with 10 dB Gaussian noise (overall noise = 7.6 dB).

A quantitative measure of the image quality is performed using four well-defined quality metrics such as MSE (mean squared error), PSNR (peak signal-to-noise ratio), MSSIM (mean structural similarity) [19], and BLUR [20]. Table 1 shows the performance of Lee filter in terms of quality metric in the proposed framework both

Table 1 Quality metrics of Lee filter output under combined speckle and Gaussian noise (overall SNR 17.6 dB)

Lee	Filtering before scan conversion	Filtering after scan conversion	Filtering with scan conversion (2 pass)	Filtering with scan conversion (1 pass)
MSE	1090.19	1363.12	652.47	1162.47
PSNR	17.79	16.82	20.02	17.51
MSSIM	0.8375	0.7911	0.8949	0.8285
BLUR	0.2541	0.2837	0.3492	0.2493

in pass1 and pass2 (Lee filter in both directions) over the two conventional filtering techniques. It is found that filtering scan conversion (2 pass) gives the best performance in terms of MSE, PSNR, MSSIM, and BLUR.

As compared to filtering before and after scan conversion, the proposed method achieves a PSNR improvement of 2.23 dB and 3.2 dB, respectively.

The proposed algorithm also employs four combinations of spatial linear and nonlinear filters in the two paradigms of speckle filtering scan conversion such as Lee-Kuan, Lee-Med, Med-Lee, and Med-Med. 'Lee-Kuan' indicates Lee filtering in radial direction and Kuan filtering in horizontal direction. The same notation is followed for other filter combinations also. Med is indicating median filter. Performance of these filtering combinations in the proposed framework is also compared with two prominent speckle reduction filters, HMM and OBNLM, as shown in Table 2. In terms of MSE and PSNR, 'Lee-Kuan' achieves the best performance with an improvement of 7.75 in MSE and a significant improvement in PSNR can be achieved with respect to 'Lee-Med' that attains the second best performance. The PSNR for HMM and OBNLM is as low as compared to 'Lee-Kuan,' 'Lee-Med,'

Table 2 Quality metrics of different filtering combinations for the noise levels

MSE						
Noise level (dB)	Lee-Kuan	Lee-Med	Med-Lee	Med-Med	HMM	OBNLM
17.6	650.0608	657.8171	678.9877	781.004	1287.915	1253.893
12.6	748.2261	820.9659	1064.882	1350.91	2007.842	2016.524
7.6	806.7585	968.2591	1661.91	2277.55	3067.872	3092.939
PSNR						
Noise level (dB)	Lee-Kuan	Lee-Med	Med-Lee	Med-Med	HMM	OBNLM
17.6	20.0329	20.0101	19.837	19.2351	17.0822	17.1965
12.6	19.4772	19.1384	17.9217	16.9198	15.1552	15.132
7.6	19.1112	18.32	15.9784	14.5926	13.2762	13.244
MSSIM						
Noise level (dB)	Lee-Kuan	Lee-Med	Med-Lee	Med-Med	HMM	OBNLM
17.6	0.8849	0.8636	0.8708	0.8399	0.847	0.847
12.6	0.8246	0.797	0.7923	0.7509	0.7048	0.7088
7.6	0.7324	0.6996	0.6686	0.625	0.5782	0.5743
BLUR						
Noise level (dB)	Lee-Kuan	Lee-Med	Med-Lee	Med-Med	HMM	OBNLM
17.6	0.384	0.2782	0.3767	0.2553	0.2959	0.3142
12.6	0.349	0.2521	0.337	0.2305	0.247	0.2547
7.6	0.3086	0.2249	0.2985	0.2068	0.223	0.2224

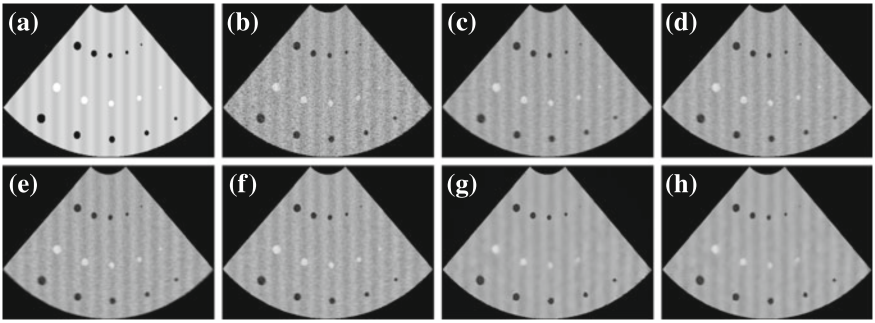

Fig. 3 **a** Original image **b** noisy image, overall noise 17.6 dB (speckle $\sigma = 1.0$, Gaussian = 20 dB) **c** Lee-Kuan **d** Lee-Med **e** Med-Lee **f** Med-Med **g** HMM **h** OBNLM filter output for speckle parameter $\sigma = 1.0$ combined with 20 dB Gaussian noise (overall noise 17.6 dB)

'Med-Lee,' and 'Med-Med.' The output images (for 17.6 dB overall noise) for different filtering combinations are represented in Fig. 3. Figure 4 shows the plot of the quality metric for three levels of noise. Table 3 depicts the real-time application of the proposed framework in terms of normalized mean time and variance, and Table 4 shows the running time of HMM and OBNLM on the scan-converted image. Filtering scan conversion examined with real scan data of ultrasound machine is given in Fig. 5.

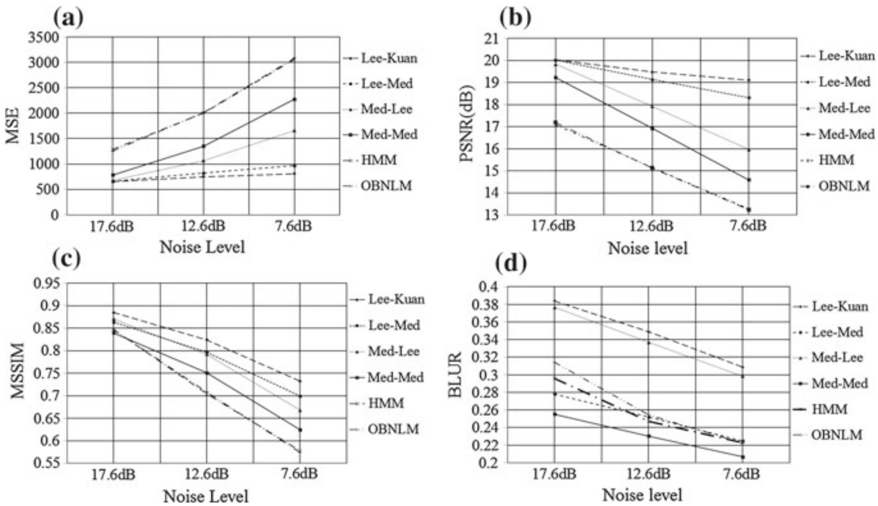

Fig. 4 **a** MSE **b** PSNR **c** MSSIM **d** BLUR at overall input SNR 17.6 dB (speckle noise $\sigma = 1.0$ added with 20 dB Gaussian noise), 12.6 dB (speckle noise $\sigma = 1.5$ added with 15 dB Gaussian noise), and 7.6 dB (speckle noise $\sigma = 2.0$ added with 10 dB Gaussian noise.)

Table 3 Normalized mean time (s) and variance of the filtering techniques in different paradigms

	Filtering before scan conversion		Filtering after scan conversion		Filtering with scan conversion	
	Normalized mean time	Variance	Normalized mean time	Variance	Normalized mean time	Variance
Lee-Kuan	0.989483	0.004642	0.695837	0.030766	0.826098	0.007313
Lee-Med	0.9892935	0.004867	0.721017	0.029154	0.839843	0.010799
Med-Lee	0.976750	0.004573	0.652359	0.017553	0.825114	0.004467
Med-Med	0.979409	0.010550	0.678938	0.022477	0.8522706	0.007719

Table 4 Normalized mean time (s) and variance of HMM and OBNLM filtering techniques

	Normalize mean time	Variance
HMM	0.56408	0.005993
OBNLM	0.41979	0.001993

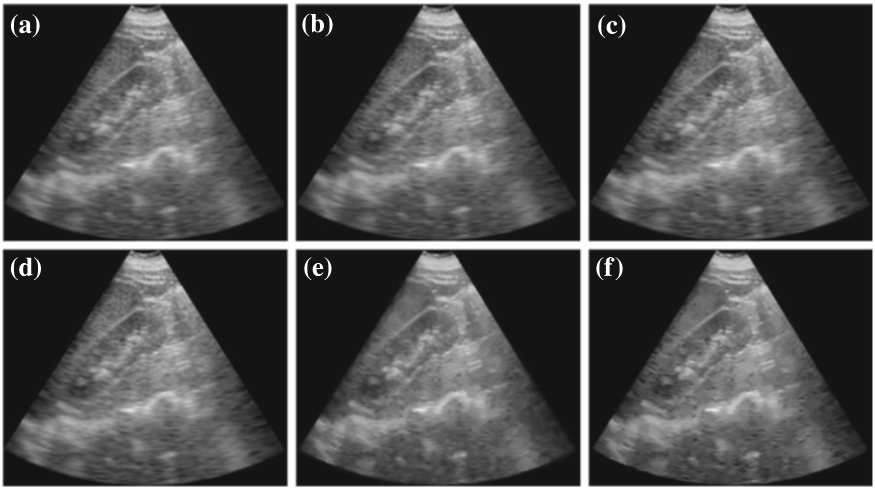

Fig. 5 **a** Lee-Kuan **b** Lee-Med **c** Med-Lee **d** Med-Med **d** HMM **e** OBNLM Filter output obtained from scan data of real ultrasound machine

6 Conclusion

Despite speckle filtering in pre- or post-processing stages, the article presents a novel framework of speckle suppression where filtering and scan conversion are unified as a single operation. The image quality metric justifies the proposed methods' efficiency when compared with other two techniques. The proposed algorithm is also compared with the two speckle reducing techniques lying in the state of the art: HMM and OBNLM. Though the image output of HMM and OBNLM looks less noisy but the fine details are found absent. On concluding the results in terms of running time of the algorithm, filtering with scan conversion takes comparable time with respect to other frameworks. Though HMM and OBNLM takes less time than the proposed technique but there is a high prospect of object loss as it is visualized from Figs. 3 and 5. The proposed algorithm is therefore well-suited with the real-time application of ultrasound imaging system with enhanced output images.

References

1. Goodman, J.W.: Some fundamental properties of speckle. J. Opt. Soc. Am. 66, 1145–1150 (1976)
2. Michailovich, O.V., Tannenbaum, A.: Despeckling of Medical Ultrasound Images. IEEE Transactions on Ultrasonics Ferroelectrics and Frequency Control. 53(1), 64–78 (2006)
3. Lee, J.S.: Refined Filtering of Image Noise Using Local Statistics. Computer Graphics and Image Processing. 15(1), 380–389 (1981)
4. Bamber, J.C., Daft, C.: Adaptive filtering for reduction of speckle in ultrasonic pulse-echo images. Ultrasonics. 24(1), 41–43 (1986)
5. Kuan, D.T., Sawchuk, A.A., Strand, T.C., Chavel, P.: Adaptive restoration of images with speckle. IEEE Transactions Acoustics. Speech and Signal Processing. 35(3), 373–383 (1987)
6. Loupas, T., McDicken, W.N., Allan, P.L.: An Adaptive Weighted Median Filter for Speckle Suppression in Medical Ultrasonic Images. IEEE Transactions on Circuits and Systems. 36(1), 129–135 (1989)
7. Dutt, V., Greenleaf, J.F.: Adaptive speckle reduction filter for log compressed B-scan images. IEEE Transactions on Medical Imaging. 15(6), 802–813 (1996)
8. Perona, P., Malik, J.: Scale-Space and Edge Detection Using Anisotropic Diffusion. IEEE Transactions on Pattern Analysis and Machine Intelligence. 4(7), 629–639 (1990)
9. Krissian, K., Fedrij, C.: Oriented Speckle reducing aniosotropic diffusion. IEEE Transactions on Image Processing. 16(5), 1412–1424 (2007)
10. Donoho, D.L.: De-Noising by Soft-Thresholding. IEEE Transactions on Information Theory. 41(3), 613–627 (1995)
11. Gleich, D., Datcu, M.: Wavelet-Based SAR Image Despeckling and Information Extraction Using Particle Filter. IEEE Transactions on Image Processing. 18(10), 2167–2184 (2009)
12. Behar, V., Adam, D., Friedman, Z.: A new method of spatial compounding imaging. Ultrasonics. 41(5), 377–384 (2003)
13. Li, P.C., Chen, M.J.: Strain Compounding: A New Approach for speckle reduction. IEEE Transactions on Ultrasonics Ferroelectrics and Frequency Control. 49(1), 39–46 (2002)
14. Buades, A., Coll, B., Morel, J.M.: A non-local algorithm for image denoising. Computer Vision and Pattern Recognition. CVPR. IEEE computer Society Conference. 2, 60–65 (2005)
15. Coupe, P., Hellier, P., Kervrann, C., Barillot, C.: Nonlocal Means-Based Speckle Filtering for Ultrasound Images. IEEE Transactions on Image Processing. 18, 2221–2229 (2009)
16. Foucher, S.: SAR image Filtering via learned dictionaries and sparse representations. Geoscience and Remote sensing symposium. IGARSS. IEEE International. 1, I-229–I-232 (2008)
17. Czerwinski, R. N., Jones, D. L., OBrien, Jr. W. D.: Ultrasound Speckle Reduction by Directional Median Filtering'. IEEE Proceedings. International Conference on Image Processing. 1, 358–361 (1995)
18. Gungor, M.A., Karagoz, I.: The homogeneity map method for speckle reduction in diagnostic ultrasound images. Measurement: Journal of the International Measurement Confederations. 68, 100–110 (2015)
19. Wang, Z. and Bovik, A. C.: Image quality Assessment: From Error Visibility to Structure Similarity, IEEE Trans. on Image Processing. 13(4), 600–612 (2004)
20. Crete, F., Dolmiere, T., Ladret P., Nicolas M.: The Blur Effect: Perception and Estimation with a New No-Reference Perceptual Blur Metric. SPIE Electronic Imaging Symposium Conf Human Vision and Electronic Imaging. San Jose:tats-Unisd'Amrique (2007)